CHAPTER 7

RESILIENT RESPONSE OF PAVEMENTS WITH CEMENTITIOUS LAYERS

CONTENTS PAGE

7.1 INTRODUCTION 7.3

7.2 ROAD SURFACE DEFLECTION 7.3

7.2.1 Deep pavement (Road 1932, Rooiwal) 7.3
7.2.2 Shallow pavement (Road 2212, Bultfontein) 7.6

7.3 MULTI - DEPTH DEFLECTION PROFILES 7.8

7.3.1 Effect of MDD hole on deflection 7.8
7.3.2 Depth - deflection behaviour 7.9

7.3.2.1 Deep pavement 7.9
7.3.2.2 Shallow pavement 7.14

7.4 EFFECTIVE ELASTIC MODULI 7.14

7.4.1 Background 7.14
7.4.2 Deep pavement 7.20
7.4.3 Shallow pavement 7.22
7.4.4 Comparison between the base moduli of the two types of pavement 7.22

7.5 TENSILE STRAIN ANALYSIS 7.25

7.5.1 Deep pavement 7.25
7.5.2 Shallow pavement 7.28
7.5.3 Fatigue life determination 7.30
7.5.4 Maximum tensile strain 7.32

7.6 VERTICAL COMPRESSIVE ELASTIC STRAIN 7.33

7.6.1 Vertical compressive strain profiles 7.33
7.6.2 Vertical strain behaviour 7.37
7.6.3 Vertical strain and permanent deformation 7.37

7.7 EFFECT OF MOISTURE INGRESS 7.40

7.8 SUMMARY AND CONCLUSIONS 7.44

7.9 REFERENCES 7.47

7.1 INTRODUCTION

In Chapters 4, 5 and 6, the discussions concerned the behaviour and evaluations related to permanent changes in both the deep (Road 1932, Rooiwal) and the shallow (Road 2212, Bultfontein) pavement. This included permanent (plastic) deformation, compression failure (crushing) and fatigue cracking. In this study the term "deflection" is used to describe resilient response, while "deformation" is used to describe permanent or plastic yield or rutting of the pavement layers.

In this chapter the resilient responses of these two types of pavements are summarised. The resilient response of pavements is a well-known indicator of pavement behaviour, similar to the behaviour indicators such as permanent deformation and cracking. These responses include road surface deflection (RSD) and multi-depth deflection (MDD). Radii of curvature (RC) were calculated for the surface deflection basin and are discussed. Effective elastic moduli for the different layers, back-calculated from the Multi - Depth Deflectometer (MDD) (De Beer et al, 1988), at various stages of trafficking, are summarised. Finally, an analysis of the tensile and vertical compressive strains using a quasi-elastic approach, is given.

The emphasis in this chapter is on the behaviour of these resilient indicators as a direct result of Heavy Vehicle Simulator (HVS) traffic loading. The results of this study are also compared to the current failure criteria for both cementitious layers and subgrade layers in South Africa.

Recommendations based on the results of this study are given to improve the current fatigue failure criteria for cementitious layers and the concept of effective fatigue life of these layers is introduced.

7.2 ROAD SURFACE DEFLECTION

7.2.1 Deep pavement (Road 1932, Rooiwal)

In full-scale HVS testing in South Africa, it is normal practice to

measure the road surface deflection with the Road Surface Deflectometer (RSD), similar to the Benkelman beam (Basson, 1985). The depth deflection profile is measured with the MDD (De Beer et al, 1988).

The standard deflection is measured with the legal load limit using a 40 kN dual wheel load, with tyre pressure at 520 kPa. These measurements were made at the start of the test as well as at various stages of trafficking. In Figure 7.1 (a) the average standard (40 kN) surface deflections at various stages of trafficking on four of the test sections on the deep pavement are illustrated. Note that the sections were trafficked at different wheel loads, ie 40, 70 and 100 kN, but the indicated deflection results are only the standard 40 kN load results. The figure indicates that the initial deflection varies between 0,2 mm and 0,3 mm, with a non-linear increase with trafficking. Initially the deflection slope is steeper than later and indicates possible fatigue failure in the cemented base layer. (This fatigue behaviour will be discussed later in Paragraph 7.6). The final deflection on the sections where the trafficking load was 40 kN (HVS Section 274A4 and 275A4) varied between 0,75 mm and 0,9 mm. On the sections with the higher trafficking loads (Sections 289A4, 70 kN, and 294A4, 100 kN), the final standard deflection varied between 1,3 mm and 1,5 mm. As found with the increase in permanent deformation on these sections discussed in Chapter 4, the increase in deflection is caused by the specific failure mechanism found for the deep pavement, viz fatigue and crushing (compression) failure in the upper section of the cemented base layer. Both the initial and final deflections on this pavement are comparable to deflections found on a similar pavement during full-scale testing in Australia (Kadar, 1988).

As a direct result of the crushing in the base, the contribution of the relative deflection from this layer to the total surface deflection increases. The lower layers also contribute to higher total surface deflection, because the weakening (crushing) of the base effectively reduces the protection of the lower layers, resulting in higher deflections, stresses and strains from these layers. During this process, the effective elastic moduli in most of the layers also reduce (see Paragraph 7.5).

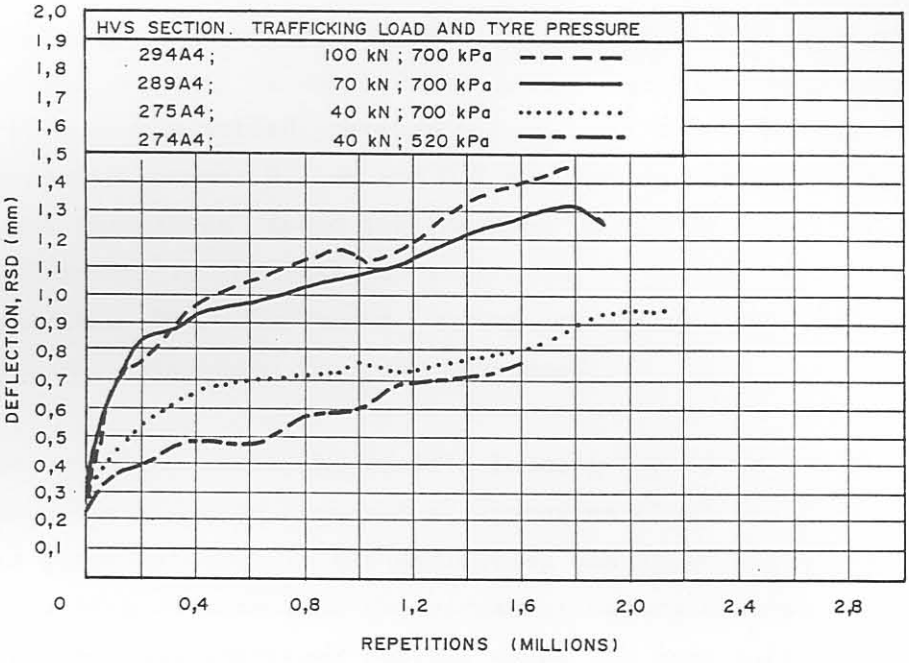

(a) DEFLECTION

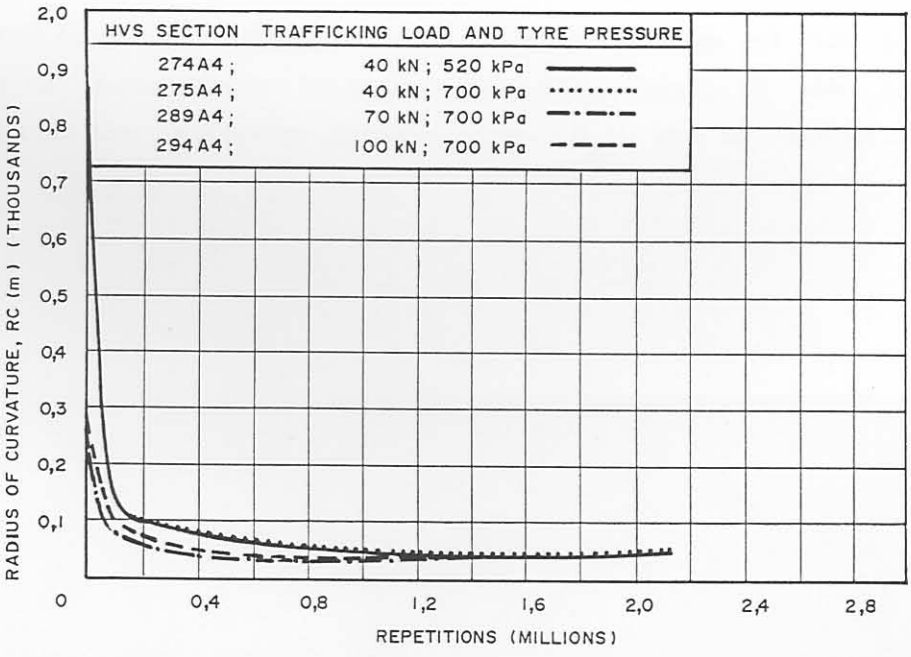

(b) RADIUS OF CURVATURE

FIGURE 7.1

SUMMARY OF THE AVERAGE STANDARD 40 kN SURFACE DEFLECTION AND RADIUS OF CURVATURE FOR THE FOUR TEST SECTIONS ON THE DEEP PAVEMENT (ROAD 1932, ROOIWAL)

In Figure 7.1 (b), the radii of curvature (RC), at various stages of trafficking on these four sections are illustrated. The figure indicates a rapid decrease in RC with trafficking from initial radii of 300 m to 850 m to a constant level of approximately 50 m, after 400 000 repetitions. The rapid decrease is indicative of structural failure in the upper layers, ie crushing of the upper section (approximately 50 - 75 mm) of the base, in this case.

These figures clearly indicate the damaging effect of the higher trafficking wheel loads in terms of both maximum deflection and curvature. The surface deflection and radius of curvature results for the individual test sections on the deep pavement, are illustrated in Appendix F, Figures F.1 and F.2.

7.2.2 Shallow pavement (Road 2212, Bultfontein)

In Figure 7.2 (a), the average standard surface deflections at various stages of trafficking on three of the HVS sections on the shallow pavement are illustrated. The deflections also increase with trafficking, similar to that found on the deep pavement. The initial deflection levels varied between 0,2 mm and 0,25 mm, while the final levels varied between 0,7 mm and 0,9 mm. These final deflection levels are lower than those found for the deep pavement, probably because of the differences in the failure mechanism. A relatively rapid increase in deflection was also noted during the first 100 000 to 200 000 repetitions, afterwhich the rate decreased.

On Section 306A4, where the traffic loading was 40 kN, another increase in standard deflection occurred at approximately 1 million repetitions. At this stage of the test the deflection was approximately 0,45 mm. It is interesting to note that the permanent deformation on the surface of this section also increased rapidly after the same amount of trafficking (see also Figure 4.8(a) in Chapter 4). Based on this result, as well as the MDD-deflections (see Paragraph 7.3), it is concluded that the cemented base layer effectively failed in fatigue at this point. The number of repetitions to introduce this change in the pavement is defined as the **effective fatigue life**, N_{ef}, and is associated with a

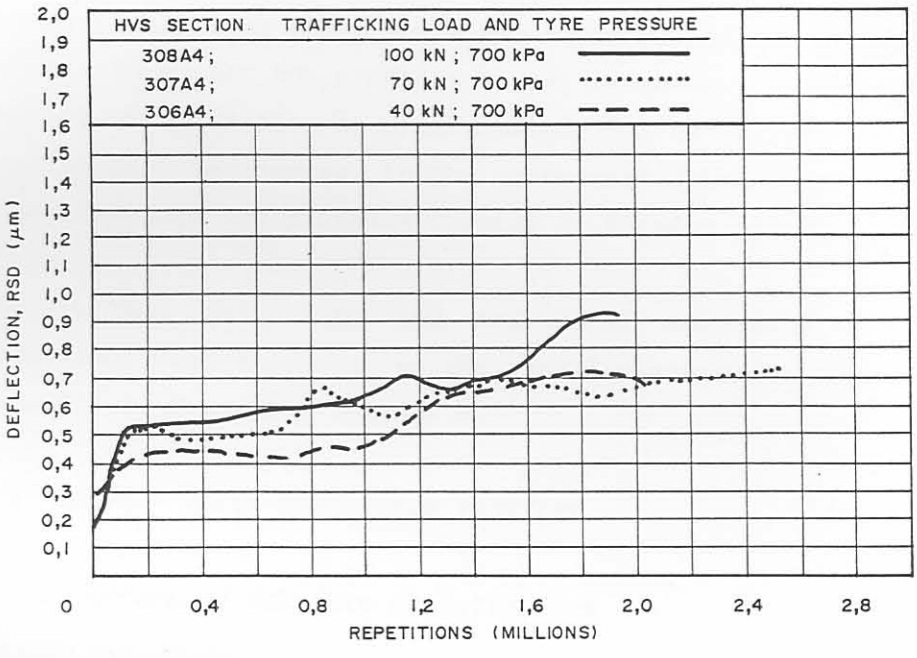

(a) DEFLECTION

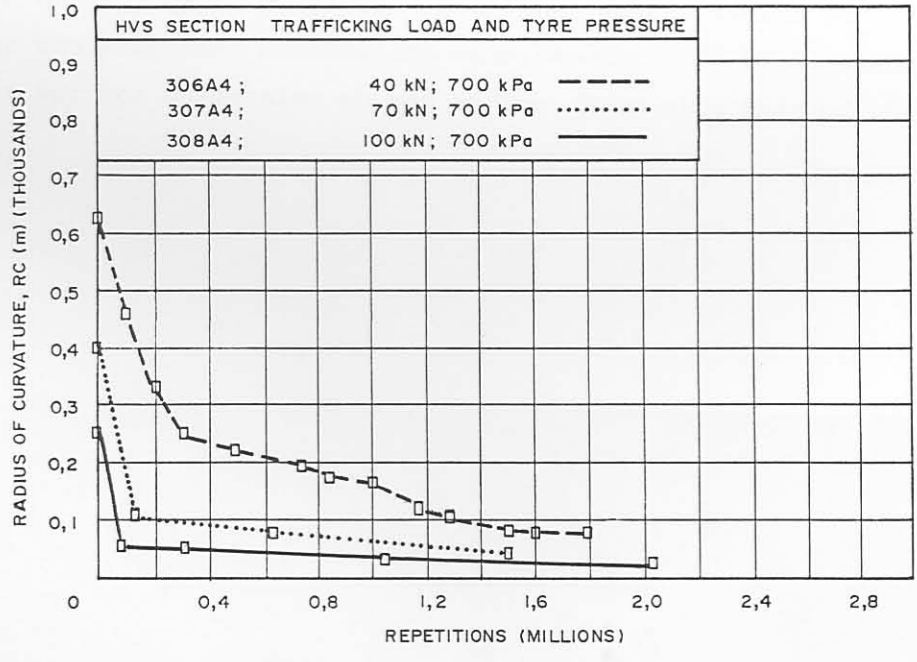

(b) RADIUS OF CURVATURE

FIGURE 7.2

SUMMARY OF THE AVERAGE STANDARD 40 kN SURFACE DEFLECTION AND RADIUS OF CURVATURE FOR THE THREE TEST SECTIONS ON THE SHALLOW PAVEMENT (ROAD 2212, BULTFONTEIN)

permanent deformation of approximately 2 mm, and a standard surface deflection between 0,5 mm and 0,75 mm. This is discussed in more detail in Paragraph 7.5.3.

In Figure 7.2 (b), the average standard (40 kN) RC values for the shallow pavement are illustrated. The figure indicates that the RC also decreases with trafficking but not as rapidly as the deep pavement. The RC changed from an original range of 600 m to 900 m, to a constant level of approximately 100 m. This is twice that found for the deep pavement and indicates that the structural failure is not associated with the base layer only, but is deeper in the pavement. In this case the subbase layer was found to be relatively weak and in an uncemented state from the start of the HVS testing (See Chapter 4, Paragraph 4.3). After the effective fatigue failure the base punched into the lower layers (see also Figure 4.15 for this mechanism) without the base layer being crushed to the same extent as that of the deep pavement. Hence the relatively higher final standard RC.

The figure also indicates the relatively higher damaging effect of the higher trafficking wheel loads in terms of surface deflection, similar to that found for the previous deeper pavement. Furthermore, the change in rate of deflection at approximately 0,5 mm is also indicated, and is similar to the changes in the permanent deformation development, as illustrated in the previous Chapter 4, Figures 4.8 and 4.9.

The surface deflection and radius of curvature results for the individual test sections on the shallow pavement, are illustrated in Appendix F, Figures F.3 and F.4.

7.3 MULTI - DEPTH DEFLECTION PROFILES

7.3.1 Effect of MDD hole on deflection

The multi - depth deflection profiles were measured with the MDDs. As for the permanent deformation measurements, it is important to compare the surface deflection on top of the MDDs with that of the rest of the

test section (between the MDDs) in order to evaluate the effect of the MDD hole on the response of the pavement during the test. This is to ensure that only representative deflection profiles are used in further analysis (in this case back-calculation of effective elastic moduli). If local failures occur at the MDD hole as a result of the disturbance of the hole in the pavement, incorrect and often over conservative deflections, and moduli, stresses and strain values result. In Figures 7.3 and 7.4 the surface deflection on the test section (omitting deflection measurements at the top of the MDDs) are compared to the deflections on the MDDs. In general, good agreement between the results exists, except for those on Sections 289A4 and 294A4, where the deflection on the MDDs were approximately 0,1 mm higher towards the end of the test. This larger deflection is most probably related to the higher trafficking wheel loads (70 and 100 kN) on these sections. Inspection during and after the HVS testing revealed slightly advanced crushing at the MDD top caps. A difference of 0,1 mm was not considered as too high. However, it is expected that the back-calculated moduli of the base layer are under estimated in these cases. Differences in these deflection levels larger than 0,1 mm are normally considered unacceptable for moduli back-calculation purposes.

7.3.2 Depth - deflection behaviour

7.3.2.1 Deep pavement

In Figure 7.5, typical depth - deflection profiles measured on the deep pavement, at various stages of HVS trafficking are illustrated. Three MDDs were installed on each HVS test section at measuring positions 4, 8 and 12. The depths of the MDD modules were located as previously indicated for permanent deformation measurements in Chapter 4 (Figure 4.3). Figure 7.5 (and Figures F.5 to F.10, in Appendix F), indicates a general decrease in deflection with depth. There was also an increase in deflection in all the layers with an increase in trafficking. The largest increase in relative deflection occurred in the base layer as a direct result of the crushing failure in the upper 50 mm to 75 mm of the base. This is well illustrated at measuring point 12 (MDD12). In Figure 7.6, the same deflection results as in Figure 7.5 are given, but in a different format, and clearly illustrate the contribution of the individual layers to the total deflection at the surface. The major

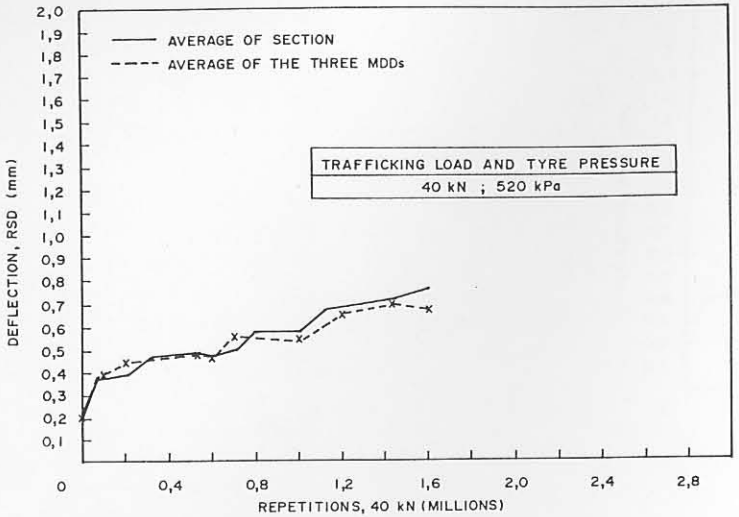

(a) SECTION 274A4

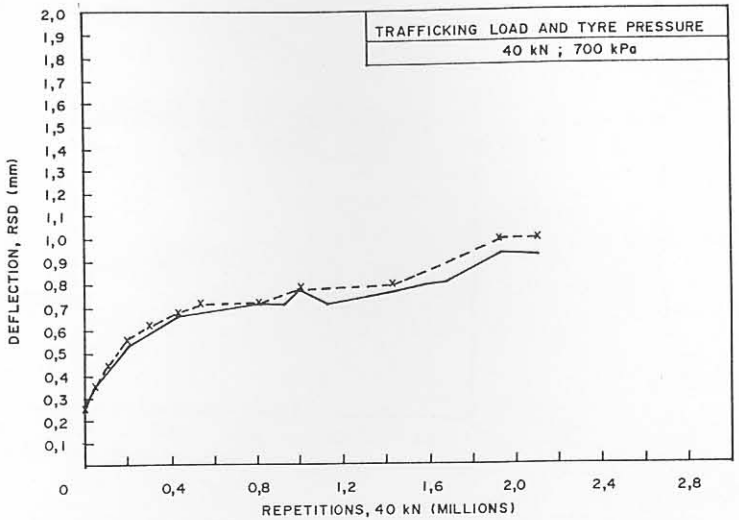

(b) SECTION 275A4

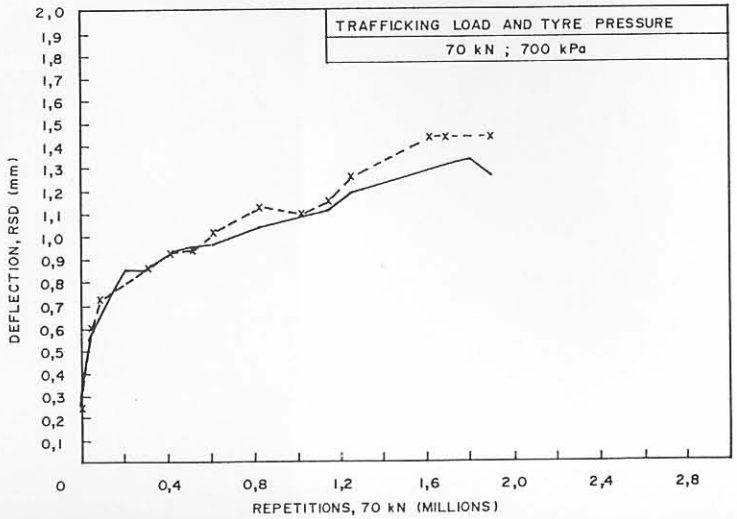

(c) SECTION 289A4

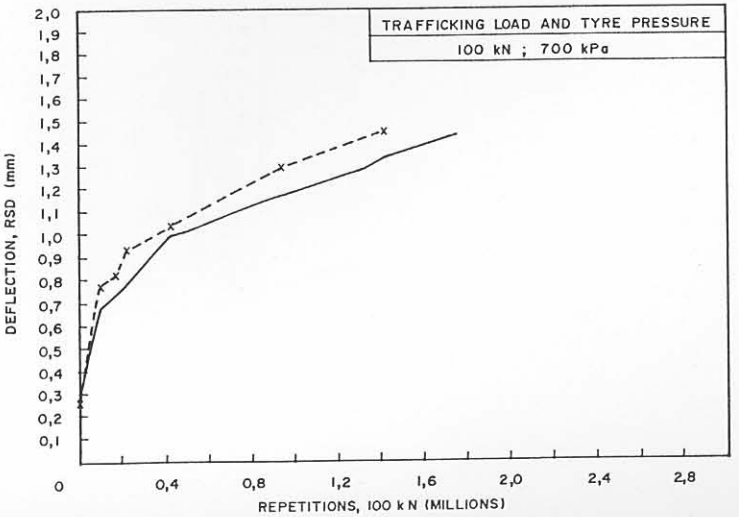

(d) SECTION 294A4

FIGURE 7.3

COMPARISON BETWEEN AVERAGE STANDARD 40 kN SURFACE DEFLECTION ON THE SECTION AND THOSE ON THE MDDs FOR THE FOUR TEST SECTIONS ON THE DEEP PAVEMENT (ROAD 1932, ROOIWAL)

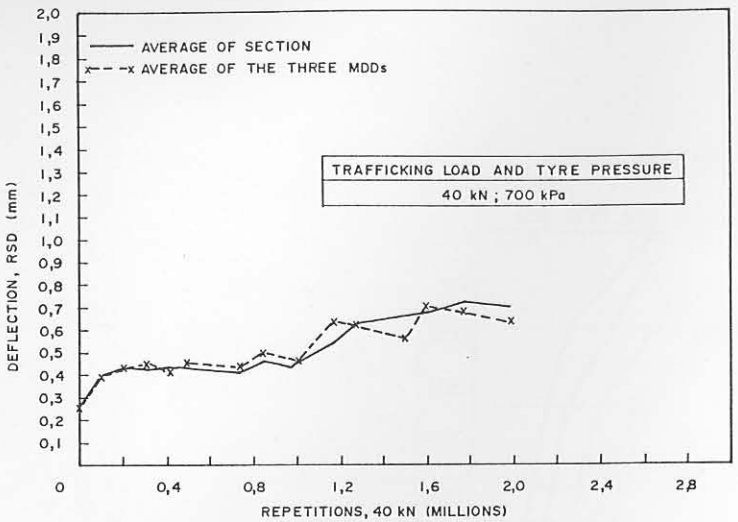

(a) SECTION 306A4

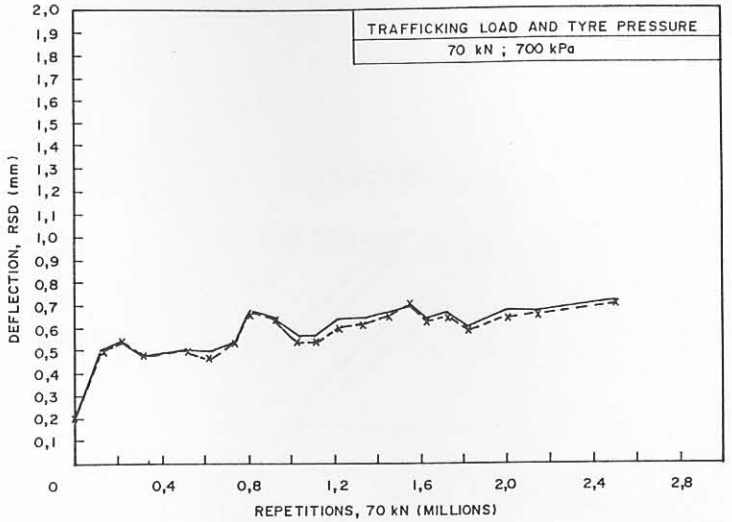

(b) SECTION 307A4

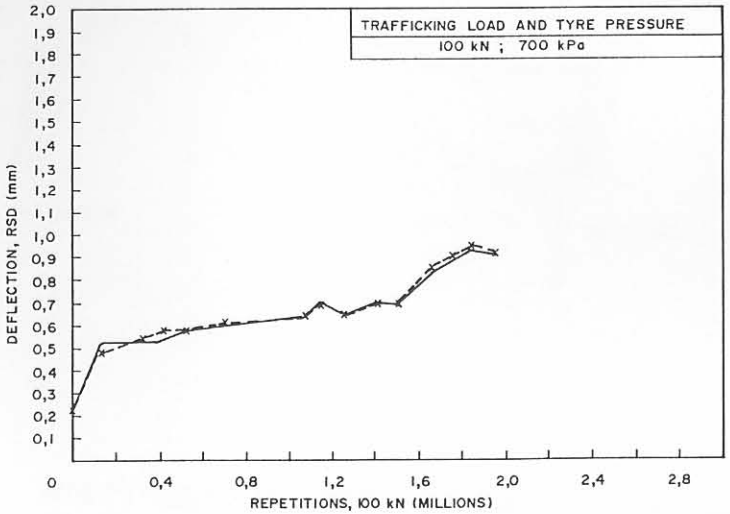

(c) SECTION 308A4

FIGURE 7.4

COMPARISON BETWEEN AVERAGE STANDARD 40 kN SURFACE DEFLECTION ON THE SECTION AND THOSE ON THE MDDs FOR THE THREE TEST SECTIONS ON THE SHALLOW PAVEMENT (ROAD 2212, BULTFONTEIN)

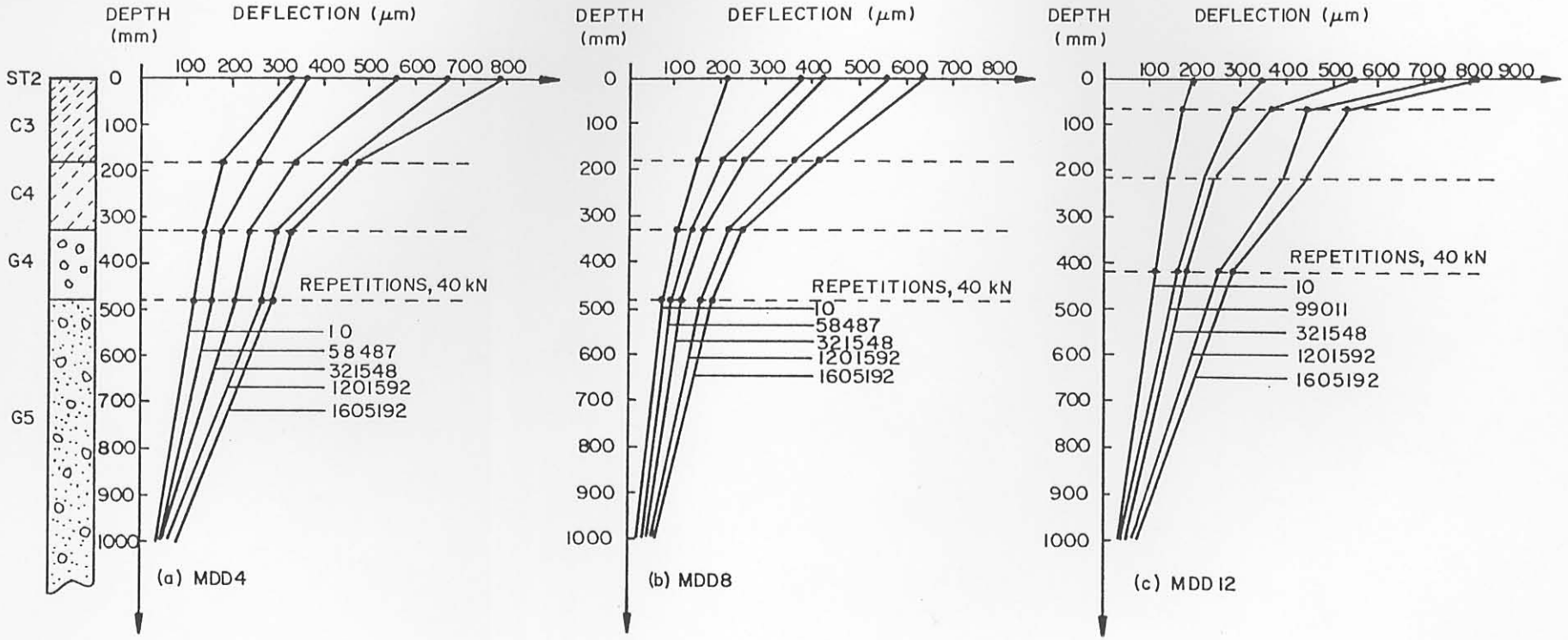

FIGURE 7.5

MULTI-DEPTH DEFLECTIONS AT MEASURING POSITIONS 4, 8 AND 12 AT VARIOUS STAGES OF TRAFFICKING ON HVS SECTION 274A4 OF THE DEEP PAVEMENT (ROAD 1932, ROOIWAL)

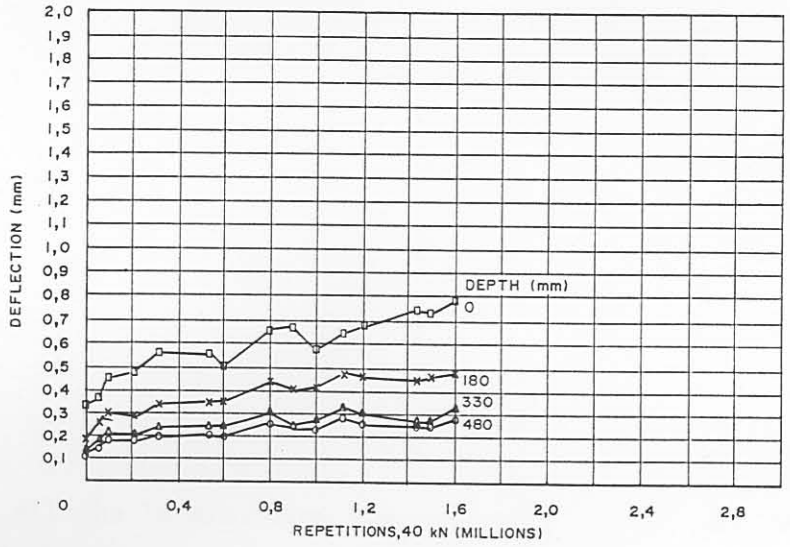

(a) MDD 4

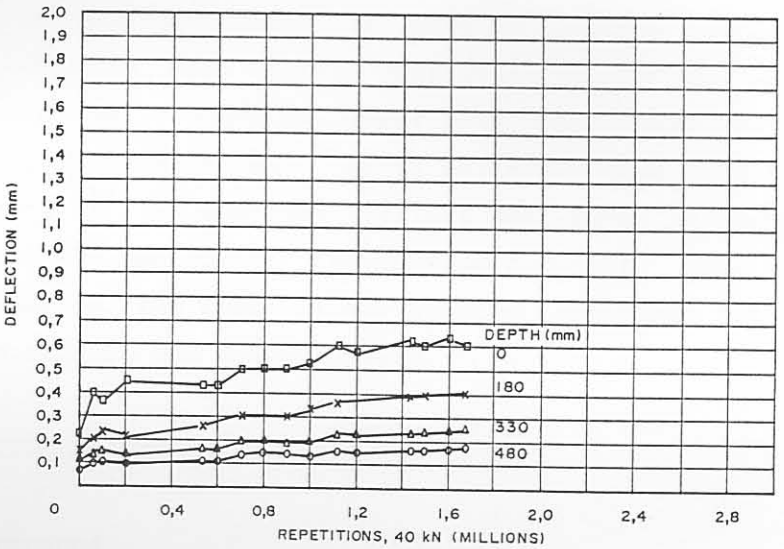

(b) MDD 8

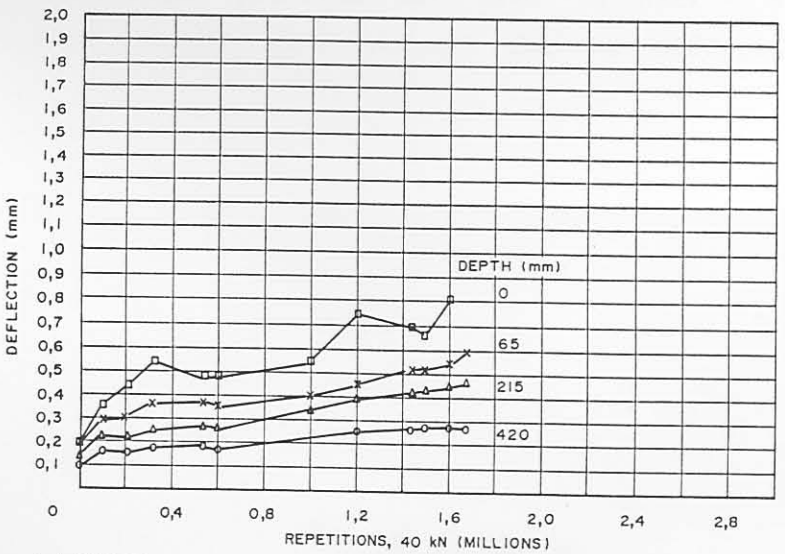

(c) MDD 12

FIGURE 7.6

AVERAGE STANDARD MDD DEFLECTION AT VARIOUS STAGES OF TRAFFICKING ON SECTION 274A4 (ROAD 1932, ROOIWAL)

portion of the total surface defection originated within the base and subgrade layers, probably exacerbated by the crushing failure in the cemented base layer.

7.3.2.2 Shallow pavement

In Figure 7.7, typical depth-deflection results from the shallow pavement are illustrated. As is the case of the deep pavement, the deflection decreases with depth, and increases as a result of traffic loading. In this case most of the deflection originates from the subgrade (480 mm downwards) and the relatively weaker subbase (110 mm to 310 mm). Figures 7.8 (a) and (c) indicate the relatively high increase in deflection (approximately 0,1 to 0,2 mm) of all the layers, at approximately 1 million repetitions (E80s), and is similar to that found with the surface deflection (see Figure 7.2). This indicates that the load bearing capacity of the base layer (0 mm to 110 mm) decreased at this point because of fatigue failure, thus transferring larger deflections to the lower layers.

In Appendix F, Figures F.11 to F.14, the increase in deflection is evident in all the layers, from the beginning of the test period. This is indicative of fatigue failure of the base from the the start of the HVS testing, under wheel loads greater than 40 kN.

Throughout the testing (except for MDD4 on Section 307A4, Figure J.12 (a), in Appendix J), the relative deflection in the base layer is small (0 mm to 0,1 mm), which is lower than that observed in the deep pavement (0,1 mm to 0,25 mm). It is believed that this is related to the difference in the dominant failure mechanism, ie crushing in the deep pavement and fatigue in the shallow pavement. Some crushing did, however, occur in the base of the shallow pavement, but to a lesser extent than that in the deep pavement.

7.4 EFFECTIVE ELASTIC MODULI

7.4.1 Background

The depth - deflection profiles were used to back - calculate the effective elastic moduli (E - values) for the different layers at

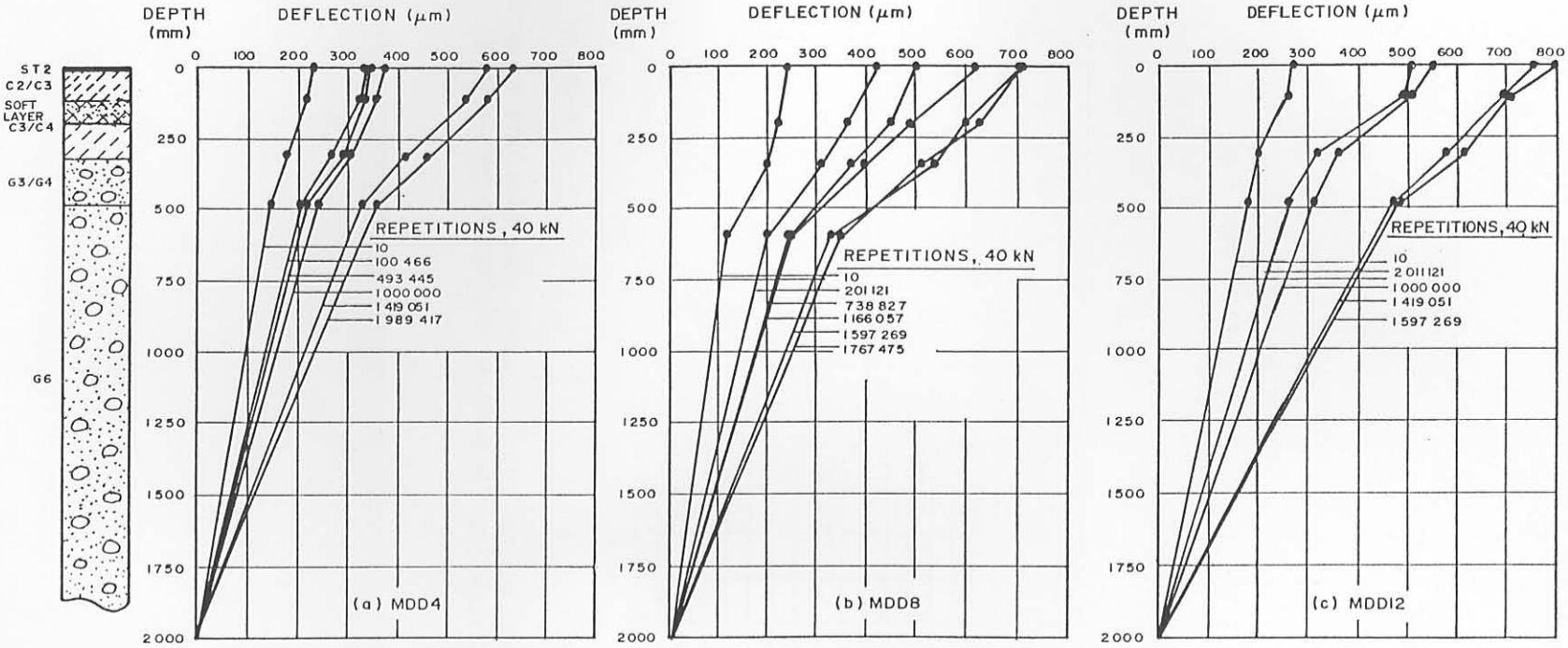

FIGURE 7.7

MULTI-DEPTH DEFLECTIONS AT MEASURING POSITIONS 4, 8 AND 12 AT VARIOUS STAGES OF TRAFFICKING ON HVS SECTION 306A4 OF THE SHALLOW PAVEMENT (ROAD 2212, BULTFONTEIN)

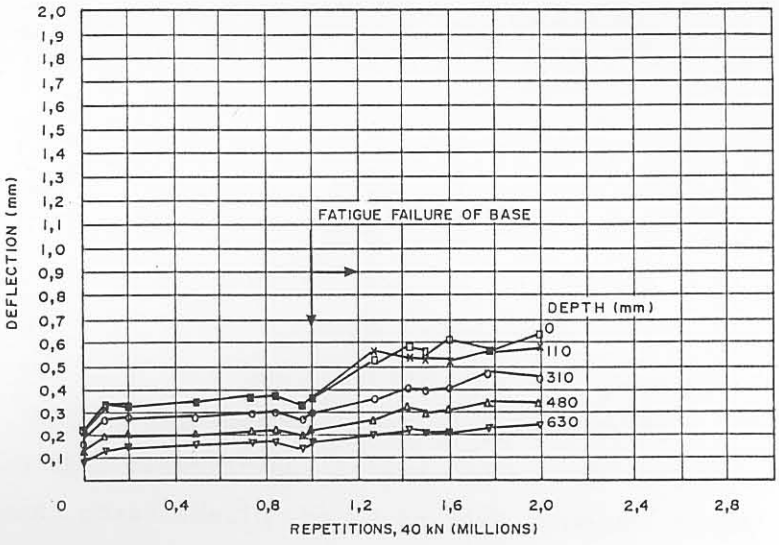

(a) MDD 4

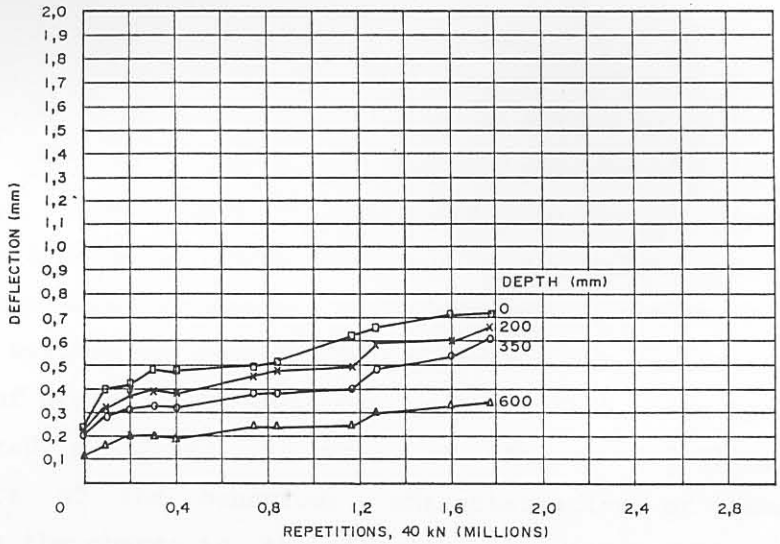

(b) MDD 8

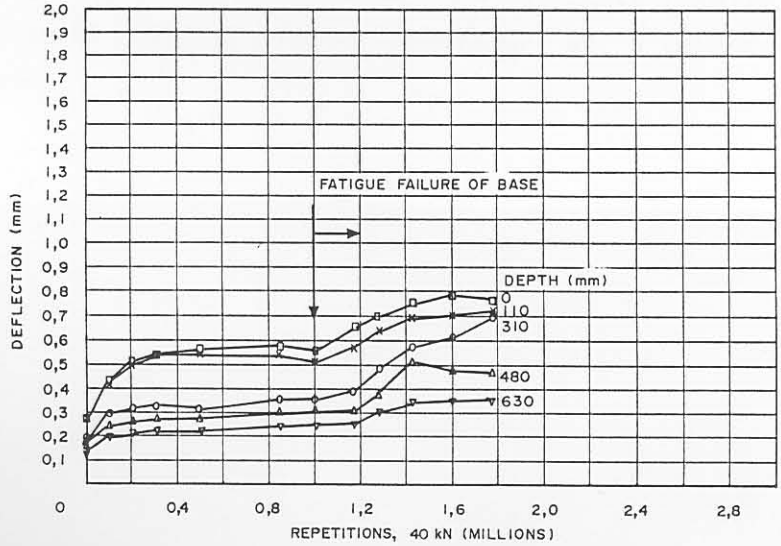

(c) MDD 12

FIGURE 7.8

AVERAGE STANDARD MDD DEFLECTION AT VARIOUS STAGES OF TRAFFICKING ON SECTION 306A4 (ROAD 2212, BULTFONTEIN)

various stages of trafficking. In this dissertation the subgrade was assumed to be of infinite depth (elastic half space), and the dual wheel loads spaced at 220 mm. The wheel spacing was smaller than that normally used, viz 350 mm, because more realistic effective moduli values were obtained for the base layers with this reduced spacing. The 220 mm spacing was fixed as twice the radius of the loaded area under standard loading conditions (40 kN, 520 kPa). It was found that unrealistically low moduli resulted for the base layers if an unloaded area between the two loads exists (350 mm spacing). It was therefore decided to reduce the spacing from 350 mm to 220 mm so that the contact areas could meet.

The results show that the moduli of all the layers decrease with trafficking, with the upper layers affected more than the lower layers. It is believed that this information on the change in moduli with trafficking will enhance the understanding of basic pavement behaviour. Over the years it has been established that the moduli, and therefore the stresses and strains in the various pavement layers, are not constant, but change because of traffic loading. It has long been recognised that cementitious layers crack and that the analysis during the cracked phase should be done with reduced moduli (Otte, 1978). Brown et al (1987) recently also indicated that data on the deterioration of the moduli of cementitious layers with time (traffic) is in short supply.

As indicated above, concepts of the reduction in moduli during the cracked phase were introduced into South Africa as early as 1978 (Otte, 1978). Freeme et al (1984) proposed the concept of "effective stiffness or moduli". For example, if a bound (bituminous or cementitious) layer cracks in fatigue or breaks down into an equivalent granular type layer, the layer ceases to behave as a homogeneous continuum in the manner normally assumed for theoretical analysis. For cementitious layers the concept of pre-cracked and post-cracked states were introduced, as is illustrated in Figures 7.9 and 7.10. Figure 7.9 illustrates several indicators of the behaviour characteristics of cemented layers, including the change in the effective elastic moduli. In Figure 7.10 (a), the conceptual reduction in the moduli of the various qualities of cementitious layers is illustrated, and in Figure 7.10 (b), a schematic presentation of the equivalent behaviour of a cemented material is illustrated.

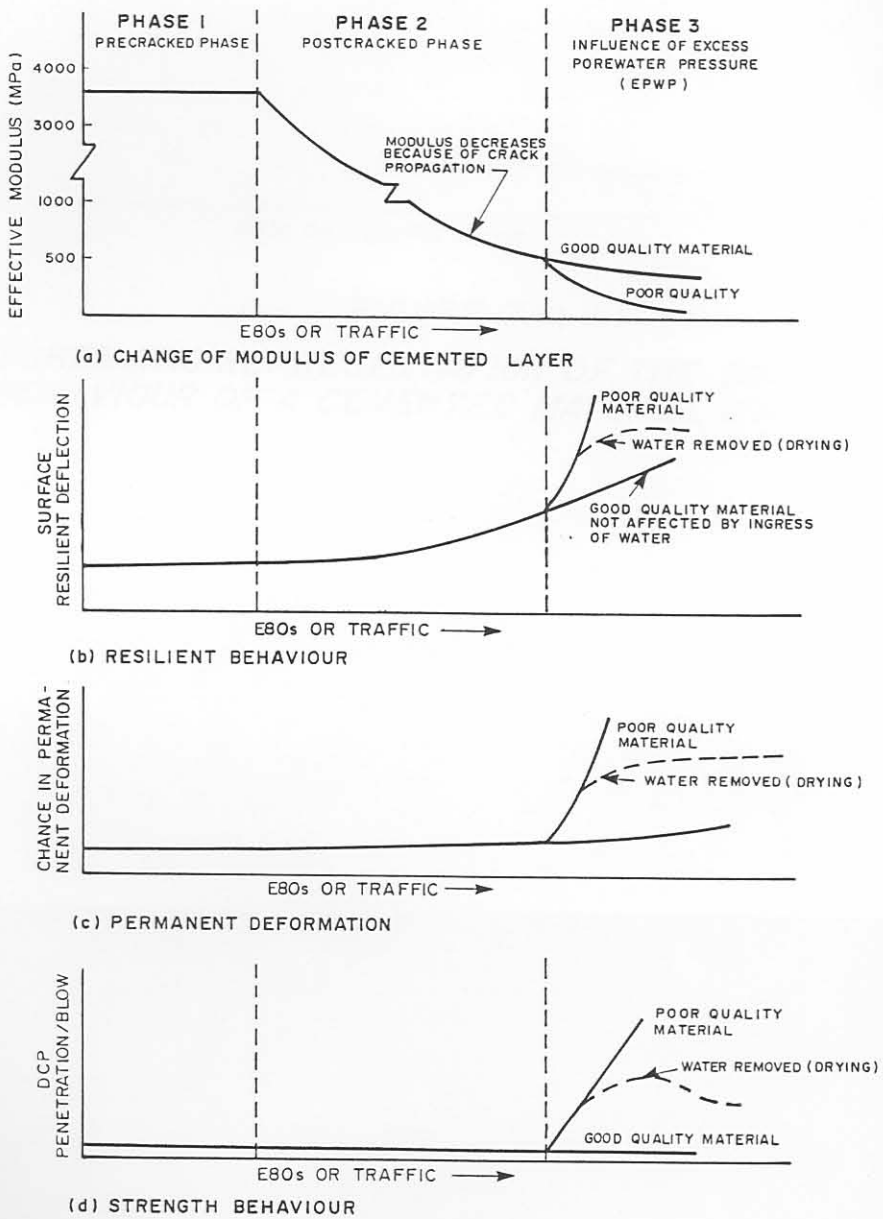

FIGURE 7.9

INDICATORS OF THE BEHAVIOUR OF CEMENTED (C2 QUALITY) LAYERS (AFTER FREEME, 1984)

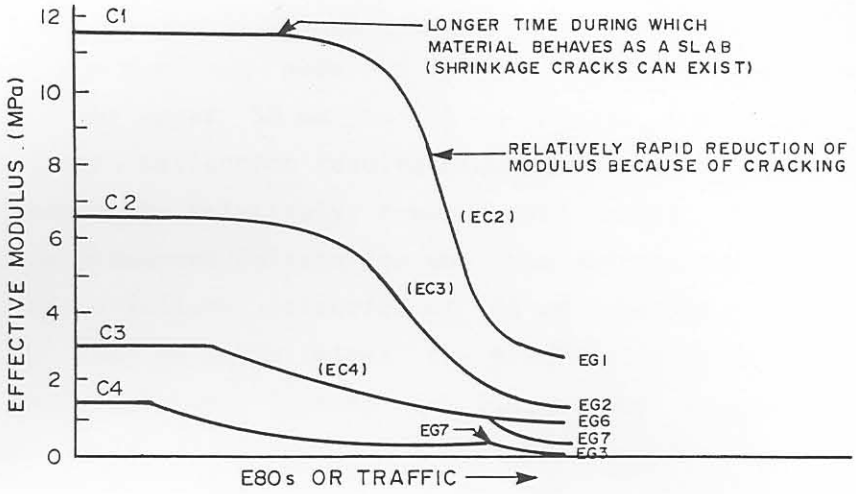

FIGURE 7.10 (a)

SHEMATIC DIAGRAM OF RELATIVE BEHAVIOUR OF CEMENTED LAYERS OF DIFFERENT QUALITY (FREEME, 1984)

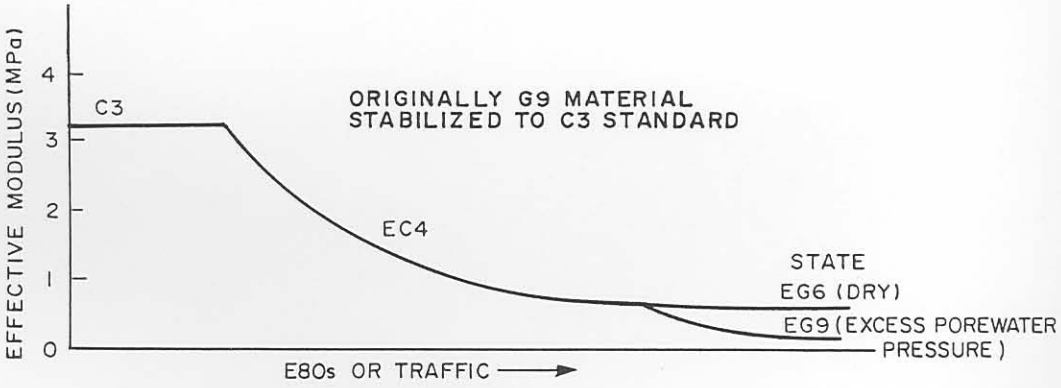

FIGURE 7.10 (b)

SCHEMATIC REPRESENTATION OF THE EQUIVALENT BEHAVIOUR OF A CEMENTED MATERIAL (FREEME, 1984)

A description of the various states of cemented layers is also given elsewhere (De Beer, 1985).

With the relatively large amount of data available from this study, it was possible to quantify the reduction in moduli of the cementitious base layers for both the deep and shallow pavements tested.

7.4.2 Deep pavement

In Figure 7.11 (a), the change in the moduli of the base (0 mm to 180 mm) for the deep pavement is illustrated, together with a reasonable (R^2 = 63 per cent) hyperbolic regression function describing the reduction. The figure indicates a rapid breakdown in the moduli from an initial range of 850 MPa to 1100 MPa, to a constant range of approximately 200 MPa to 300 MPa. Laboratory determined moduli on intact specimens of the base material varied between 1300 MPa and 1995 MPa. In Figure 7.11 (b), upper and lower limits for the found range of moduli are also given. From these figures it is evident that the cementitious base converts rapidly to an equivalent granular state. In this case, as described in Chapter 4, the dominant mode of failure on this deep pavement was crushing in the upper 50 mm to 75 mm of the base. This was also reflected in the deflection results discussed in Paragraphs 7.2 and 7.3. Notwithstanding the relatively lower moduli during the crushed state, the absolute permanent deformation on this pavement was relatively low and based on a failure criterion of 20 mm rutting. These pavements could carry two to three times the traffic originally anticipated, provided that moisture ingress is limited by regular sealing and maintenance.

In an earlier study it was indicted that the the reduction in effective moduli of cementitious subbase layers in bituminous base pavement structures is not as rapid as those of the base layers discussed here (De Beer, 1985). This is due to the fact that the bituminous base layer absorbs most of the severe stresses and not the deeper cemented subbase layers.

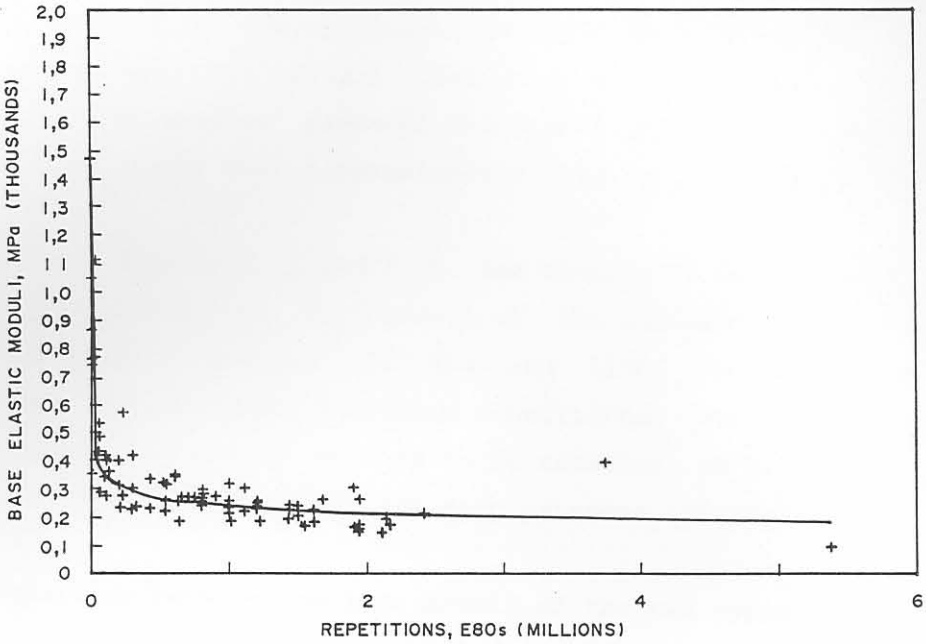

(a) AVERAGE REGRESSION

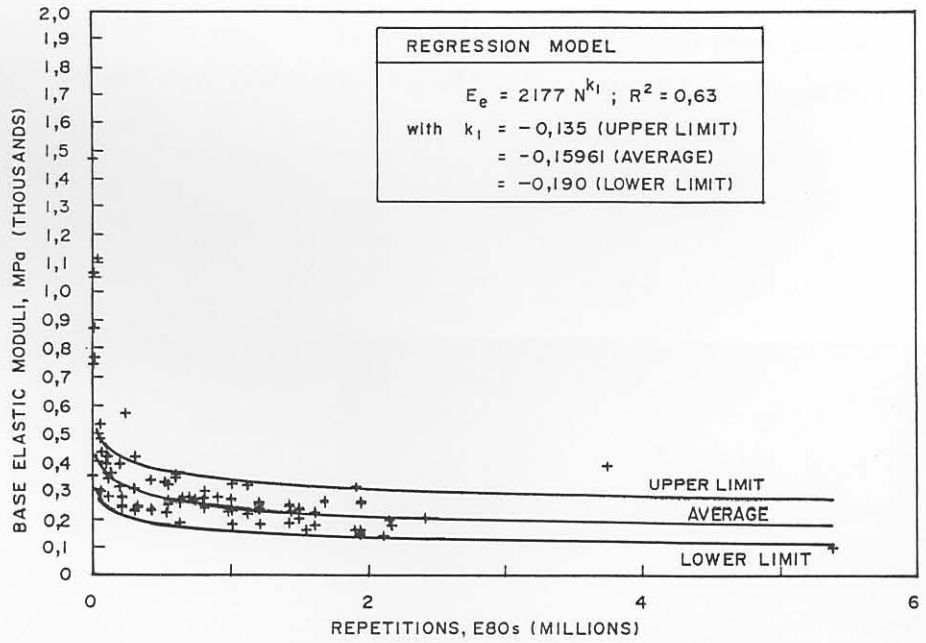

(a) AVERAGE REGRESSION WITH UPPER AND LOWER LIMITS

FIGURE 7.11

RELATIONSHIPS BETWEEN THE MDD BACK-CALCULATED EFFECTIVE ELASTIC MODULI OF THE BASE AND NUMBER OF EQUIVALENT 80 kN AXLES, ON THE DEEP PAVEMENT (ROAD 1932, ROOIWAL)

The moduli of the lower layers also decreased with an increase in trafficking. In Appendix F, Figures F.15 and F.16, the reduction in moduli of the subbase, selected and subgrade layers, are illustrated. For the selected layer the moduli were relatively high, and variable, without a distinct decrease notable. The reason for this is not clear, but it is possible that interference between the cemented subbase and the top of selected layer as a result of debonding may have contributed to this effect. The final moduli of the lower layers appears to be approximately 50 MPa.

7.4.3 Shallow pavement

In Figure 7.12 (a) and (b), the decrease in moduli of the base layer (0 mm to 110 mm) of the shallow pavement is illustrated. The figure illustrates greater variability compared to that of the deep pavement, but the average breakdown may also be described by an hyperbolic function (R^2 = 34 per cent). The moduli reduced from an initial range of 2250 MPa to 3400 MPa to a final range of approximately 500 MPa. This is larger than for the deep pavement, possibly because of the different failure mechanisms. The initial laboratory determined modulus for the base layer of the shallow pavement was also higher (approximately 5580 MPa) than that of the deep (approximately 1300 to 1995 MPa) pavement.

In Appendix F, Figures F.17 and F.18, the changes in moduli of the lower layers, are illustrated. The moduli of the subbase layer initially varied considerably between 430 MPa and 1150 MPa and reduced to approximately 100 MPa after 4 million repetitions. For the selected and subgrade layers the moduli appears to be constant at 100 MPa, and are also higher than that found for the deep pavement (50 MPa).

7.4.4 Comparison between the base moduli of the two types of pavement

In Figure 7.13(a) and (b), the change in moduli of the two pavements, are illustrated. The figures indicate the "intact state" together with the distressed state. From the results of this study it appears that distinction should be made between the type of distressed state of these pavements, because the reduction in effective moduli is directly related

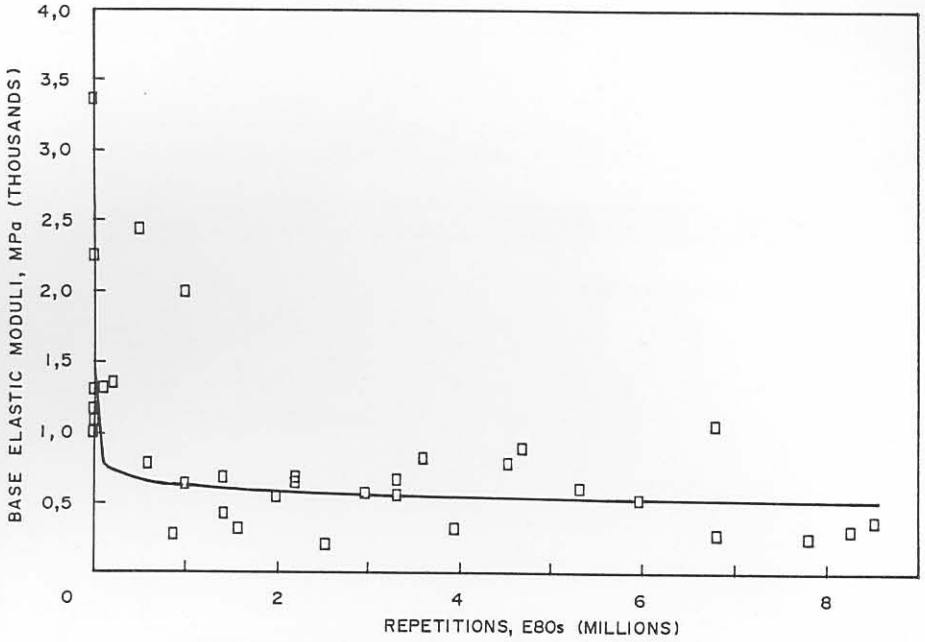

(a) AVERAGE REGRESSION

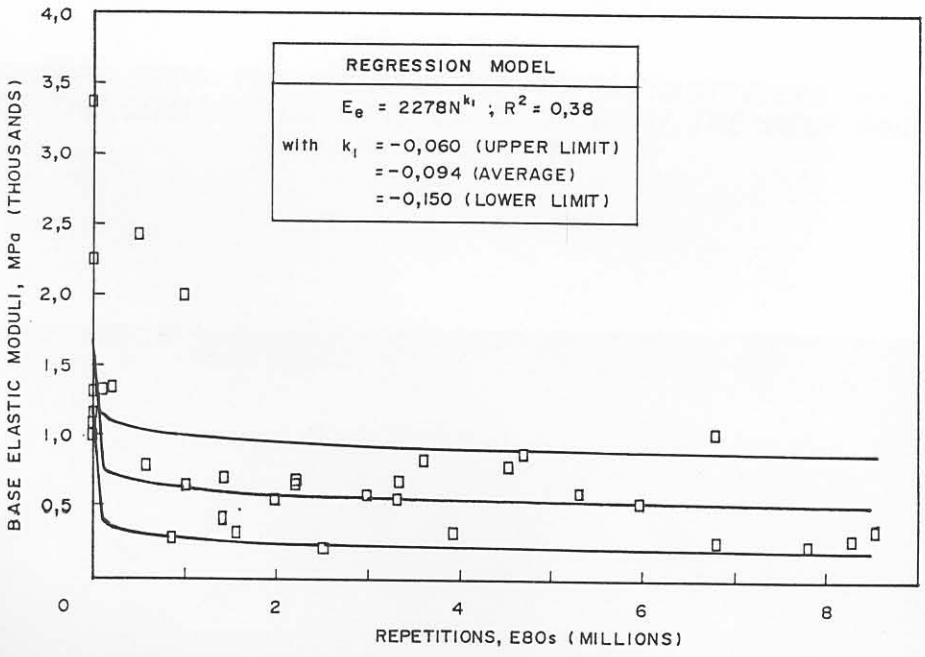

(b) AVERAGE REGRESSION WITH UPPER AND LOWER LIMITS

FIGURE 7.12

RELATIONSHIPS BETWEEN MDD-CALCULATED EFFECTIVE ELASTIC MODULI OF THE BASE AND NUMBER OF EQUIVALENT 80 kN AXLES, ON THE SHALLOW PAVEMENT (ROAD 2212, BULTFONTEIN)

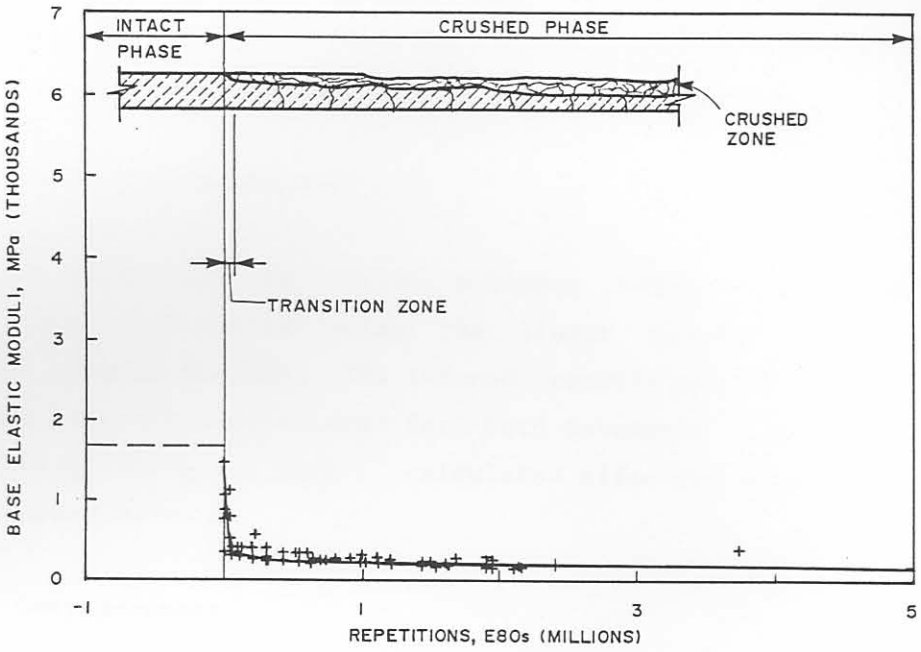

(a) DEEP PAVEMENT (ROAD 1932, ROOIWAL)

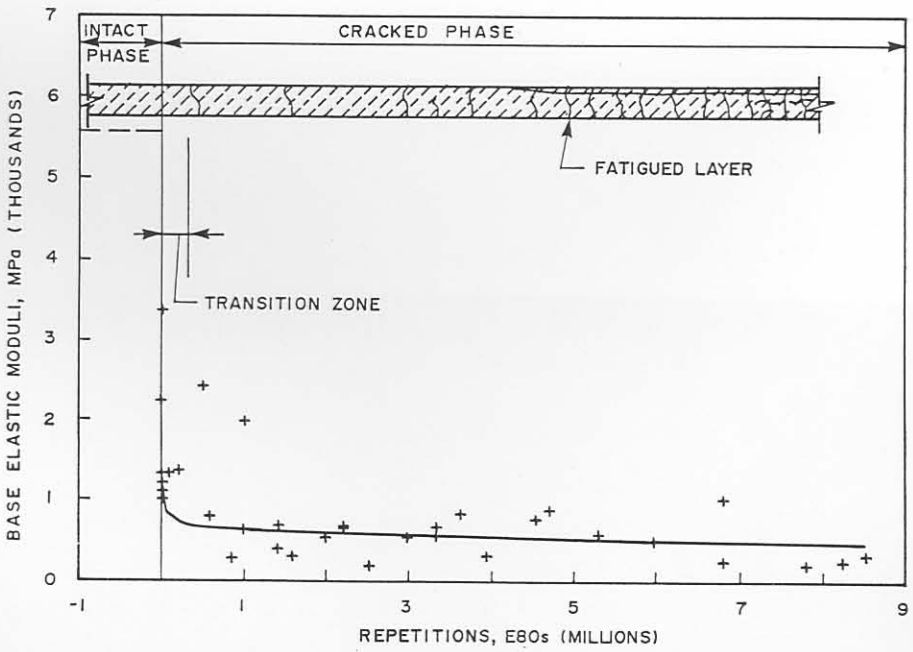

(b) SHALLOW PAVEMENT (ROAD 2212, BULTFONTEIN)

FIGURE 7.13

CHANGE FROM THE INTACT PHASE TO THE DISTRESSED PHASE OF THE CEMENTITOUS BASE LAYER OF BOTH THE DEEP AND SHALLOW PAVEMENTS

to either crushing or fatigue failure. Conceptually the distressed state was assumed to be the post - cracked state (see Figure 7.9 (a) and Figure 7.10). For the **deep pavement** the distress in the cementitious base is manifested as **crushing**, whilst for the **shallow pavement** the distress is **fatigue**. It is therefore advisable to differentiate between these two modes of failure. For the deep pavement the two major states in its life are **intact** and **crushed**, while for the shallower pavement these states are **intact** and **cracked** (see Figures 7.13 (a) and (b)).

For both pavement types there is a transition zone between the intact and distressed states. Closer inspection of these zones indicates that the average reduction in moduli occurs within the first 30 000 repetitions (E80s) for the deep pavement, and within 100 000 repetitions (E80s) for the shallower pavement. These zones are illustrated in Figure 7.14.

In Figure 7.15 the relationships of the average change in effective elastic moduli in the distressed states of the base layers of the deep and shallow pavements are compared. This figure may be a useful design guideline for these two pavements in mechanistic design.

7.5 TENSILE STRAIN ANALYSIS

With the moduli of the various pavement layers known, stresses and strains were calculated using the linear elastic multi - layered computer program ELSYM5A. The induced tensile strain at the bottom of the base layers was calculated for both pavements at various stages of trafficking (using the back - calculated effective elastic moduli) and is discussed below.

7.5.1 Deep pavement

In Figure 7.16 (a), the change in strain ratio (ϵ_s/ϵ_b) with increase in trafficking on the deep pavement is illustrated.